Structural Characteristics and Defects in Ethyl−Cyanoethyl Cellulose/ Acrylic Acid Cholesteric Liquid Crystalline System

Linge Wang† and Yong Huang*

Laboratory of Cellulose and Lignocellulosics Chemistry, Guangzhou Institute of Chemistry, Chinese Academy of Sciences, Guangzhou 510650, P. R. China and State Key Laboratory of Polymer Physics and Chemistry, Institute of Chemistry, Chinese Academy of Sciences, Beijing 100080, P. R. China

Received April 16, 2003; Revised Manuscript Received November 12, 2003

ABSTRACT: Structural characteristics and optical properties of ethyl−cyanoethyl cellulose [(E−CE)C]/ acrylic acid (AA) cholesteric liquid crystalline solutions and their variations caused by polymerization AA were investigated by UV−vis spectroscopy and wide-angle X-ray scattering (WAXS). With increasing (E−CE)C concentration, both the pitch (*P*) and the reflection wavelength of the (E−CE)C/AA solutions decreased exponentially but the average intermolecular distance (*d*) was only slightly decreased. After photopolymerization of the solvent AA, the supramolecular structure and the reflection property of the cholesteric order of the solution were well preserved in the (E−CE)C/poly(acrylic acid) (PAA) composites. However, *P*, the reflection wavelength, and *d* were all decreased due to the volume contraction of AA. In the fractured surface of the microtomed composites (parallel to the cholesteric helical axis), a periodic lamellar structure was observed by transmission electron microscopy (TEM). A series of defects (disclinations and dislocations) were also observed and elucidated from the TEM micrographs.

Introduction

The structure of cholesteric liquid crystalline polymer (LCP) is one interesting topic in the fields of polymer science and liquid crystals. Many natural biomacromolecules can form cholesteric liquid crystalline (LC) phases such as cellulose, polypeptide, and DNA as well as a helical arrangement of the molecules formed in the cholesteric LC phase. As shown in Figure 1, in any small elements of volume, the rod-shaped molecules are arranged similarly to nematic ordering in a "layer", which the long axes of the molecules are approximately parallel along one orientation vector, and the orientation vector successively turns a small torsion angle from one layer to the next one along the helix axis, so that a supermolecular structure with helical ordering appears.[1] Derived from this helical structure, many characteristic and remarkable optical properties are shown in the cholesteric LC phase, which have potentially commercial optical applications such as polarized light sources,[2,3] information display and storage devices,[4] and "photocopy-safe" and decorative materials.[5,6] One great property among them is the selective reflection; the cholesteric LC phase can reflect one hand of circularly polarized light when the wavelength of the light coincides with the pitch (*P*) of the cholesteric phase. The relationship between the wavelength and the pitch, according to De Vries's theory,[1] can be described by the following equation

$$\lambda_{max} = nP \sin \varphi \qquad (1)$$

where λ_{max} is the maximum wavelength of the selective reflection, n is the average refractive index of the mesophase, and φ is the angle between the incident light and the ordered molecular layers in the cholesteric phase.

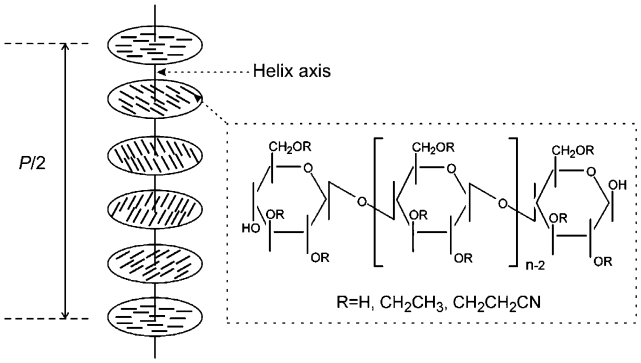

Figure 1. Schematic arrangement of the molecules in the cholesteric structure and the molecular formula of (E−CE)C.

Since Werbowyj and Gray found cholesteric LC phase in aqueous hydroxypropyl cellulose (HPC) solution in 1976,[7] many cellulose derivatives have been found that they could form lyotropic cholesteric LC phases in appropriate solvents.[8] Ethyl−cyanoethyl cellulose [(E−CE)C], which is a cellulose derivative with two different ether groups, ethyl and cyanoethyl (Figure 1), can form cholesteric liquid crystalline solution in many organic solvents, such as dichloroacetic acid (DCA)[9] and acrylic acid (AA).[10] In our previously studies, an investigation into the LC behavior of the (E−CE)C/AA LC solution has been undertaken.[10−15] Similar to other polymer lyotropic cholesteric LC solutions, the (E−CE)C/AA cholesteric LC solution shows the multitexture with variation of the concentration[10] and exhibits vivid colors in a particular high concentration range due to the selective reflection property. The critical concentration (C_1) and the pitch were influenced by the (E−CE)C molecular weight and the molecular structure, respectively.[12,15] C_1 varied inversely with both the molecular weight and the degree of substitution of cyanoethyl,[12] whereas the pitch increased with increasing molecular

* To whom correspondence should be addressed. Address: Bureau of Basic Research, Chinese Academy of Sciences, 52 Sanlihe Road, Bejing 100864, P. R. China. Phone: +86-10-68597350. Fax: +86-10-68597356. E-mail: yhuang@cashq.ac.cn.
† Ph.D. candidate of the Graduate School of the Chinese Academy of Sciences. E-mail:lg-wang@mail.gic.ac.cn.

10.1021/ma0344893 CCC: $27.50
Published on Web 12/18/2003

weight and reached a minimum value when the degree of substitution of cyanoethyl was 0.25.[15] Furthermore, it was found that the cholesteric structure of the (E−CE)C/AA solution can be frozen in (E−CE)C/poly(acrylic acid) (PAA) composite by photopolymerization of the solvent AA.[11] After microtomed the (E−CE)C/PAA composite, the morphology and structure of the cholesteric order can be observed by transmission electron microscopy (TEM), low-voltage scanning electron microscopy (LVSEM), and atomic force microscopy (AFM).[11,13,14] The formation of a periodic lamellar structure, which has the typical structure of the cholesteric phase, has been observed in the fractured surface of the (E−CE)C/PAA composite. However, some questions still exist with the (E−CE)C/AA cholesteric LC system. The arrangement of the (E−CE)C molecules to form the supermolecular structure is not clear; other questions are how the structural variation (the helix axis direction, chains packing, etc.) occurs during the polymerization of the AA and how much polymerization effects the cholesteric structure? Because the volume contraction arises from the polymerization of vinyl monomers, little work has been reported comparing the cholesteric structure before and after polymerization of monomer solvent. This question also exists in other cellulose/vinyl derivative cholesteric LC systems.

In this paper, the structural characteristics and optical properties of (E−CE)C/AA cholesteric LC solutions were investigated in detail by UV−vis spectroscopy and wide-angle X-ray scattering (WAXS). The dependencies of the reflection wavelength, the pitch, and the intermolecular distance (d) with the (E−CE)C concentration and the molecular arrangement were studied and compared before and after polymerization of the AA. The defects in the (E−CE)C/AA cholesteric LC systems was also investigated.

Experimental Section

Materials. (E−CE)C was prepared by reaction of ethyl cellulose (EC) (Luzhou Chemical Plant, China) and acrylonitrile by the following procedure:[16] 20 g of EC was dissolved in 500 mL of acrylonitrile and subsequently 20 mL of 5% NaOH aqueous solution added. The reaction mixture was kept at 50 °C with continuous stirring for 4 h, and then 50 mL of 5% acetic acid was added to the mixture. The suspension mixture was then poured into distilled water at 96 °C with vigorous stirring to distill excess acrylonitrile. The product was filtered and washed with distilled water several times. The final product was dried under vacuum at 65 °C. The yield was about 75%, and the product, (E−CE)C with degree of substitution for ethyl of about 2.1 and for cyanoethyl of about 0.33, was determined by elemental analysis (CHN−O−RAPID, Heraeus, Germany). The molecular structure is shown in Figure 1. The molecular weight of (E−CE)C was measured by gel permeation chromatography (GPC), which consists of a solvent delivery system Waters model 515 HPLC pump controlled by M32 software (Water Corp.), an Ultrastyragd column (7.8 × 300 mm) with pore sizes of 10^4 Å (Water Corp.) held at 40 °C, and a differential refractometer (Water RID 410 detector). Tetrahydrofuran (THF) was used as the eluent at a flow rate of 1.0 mL/min. M_n was 0.97×10^5, and M_w was 1.90×10^5, with PD = 1.98. All reagents were chemically pure, and AA was distilled in a vacuum at 50 °C before use.

Preparation of (E−CE)C/AA Solutions and (E−CE)C/PAA Composites. (E−CE)C/AA solutions ranging from 42 to 56 wt % were prepared. An appropriate amount of (E−CE)C was mixed with AA and 2 wt % (with respect to the solvent AA) initiator, benzoin ethyl ether, at room temperature (about 20 °C). The mixture was allowed to set for about 2 weeks, and the resulting homogeneous solutions were then stored in the dark until used. The solution was sandwiched between two quartz slides and sealed with solid wax and stored in the dark for several hours. The thickness of the solution films was controlled to 0.45 mm by a Teflon spacer. Then, the solution films were inserted into an ultraviolet chamber equipped with a 250 W high-intensity mercury arc lamp for 2 min, and the (E−CE)C/PAA composites were prepared after polymerization of the AA. The distance between the lamp and the sample was 5 cm, and the polymerization temperature was 0 °C.

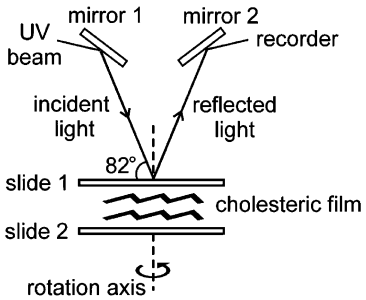

Figure 2. Apparatus setup of the UV−vis spectrophotometric method. The fixed angle between the incident light and the sample plate was 82°.

Measurements. The reflection spectra of the (E−CE)C/AA cholesteric LC solutions and the (E−CE)C/PAA cholesteric composites were measured by an UV−vis spectrophotometer (UV-2550, SHIMADZU, Japan). To investigate the variation of the direction of the helix axis, the samples were placed in a rotating sample stage, shown in Figure 2; the rotation axis is perpendicular to the slide surface. If the helix axis is perpendicular to the film surface, i.e., the molecules are in a planar texture arrangement, the angle between the incident light and the ordered molecular layers in the cholesteric phase (φ) will be fixed to 82°, and the reflection peak will keep the same shape and position with different sample rotation angles. If the helix axis is oblique to the film surface, then φ will be varied with the sample rotation and the deviation angle between the helix axis and the rotation axis can be calculated according to the wavelength data. The average refractive index of the samples was measured by an Abbe refractometer (2WA, Shanghai Optical Instrument Factory, China). The average intermolecular distance of the (E−CE)C/AA solutions and the (E−CE)C/PAA composites was measured by WAXS, using an X-ray diffractometer (D/MAX-1200, Rigaku, Japan), Cu Kα radiation ($\lambda = 1.5405$ Å), Ni filtration, scanning from $2\theta = 3°$ to 40°. As for solution samples, the (E−CE)C/AA solution was coated in a thin film (0.1 mm) in a quartz slide surface and WAXS was performed after the shearing orientation formed during coating was relaxed. Composite samples were used the photopolymerized films. The morphologies and defects of the mesophase structure were observed by a transmission electron microscope (TEM) (JEM-100CX/II, JEOL, Japan) at 100 keV, after the composite films were sectioned to ultrathin films (60−70 nm) by an ultramicrotome (LKB-208B, BROMMA, Switzerland) at room temperature. The cutting direction was perpendicular to the film surface.

Results and Discussion

Twist Structure in (E−CE)C/AA Cholesteric LC System. In polymer lyotropic cholesteric LC solution, such as polypeptides,[17,18] the birefringent phase begins to separate when a limiting concentration, C_1, is exceeded and is the only phase present when a somewhat higher concentration, C_2, is exceeded. Between these two concentrations the isotropic and the birefringent phases exist in equilibrium. For the (E−CE)C/AA solution, C_1 is 35 wt % and C_2 is 42 wt %. In the concentration range from 42 to 56 wt %, the pitch of (E−CE)C/AA cholesteric LC solutions approaches the visible light wavelength and the solutions exhibit vivid colors due to the selective reflection to visible light.[1] Figure 3a shows the reflection

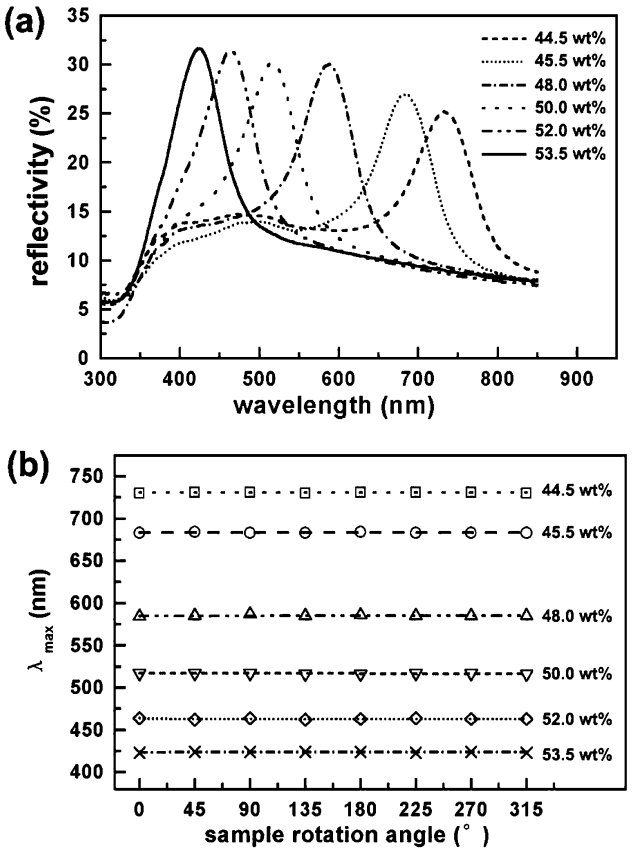

Figure 3. Reflection spectra of (E−CE)C/AA cholesteric LC solution films (a) and λ_{max} with different sample rotation angles (b).

spectra of the (E−CE)C/AA solutions, and it can be seen that λ_{max} shifts to shorter wavelengths with increases in (E−CE)C concentration. All reflection peaks of the solutions maintain the same shape and wavelength with different rotation angles (Figure 3b), and this indicates that the (E−CE)C molecules in the solutions form a very well ordered planar texture arrangment according to the explanation in the Experimental Section. As shown in Table 1, after the average refractive index (n) is measured, the pitch of the (E−CE)C/AA solutions (P_0) is calculated according to eq 1 and is a decreasing function of concentration, which is a common phenomenon among most polymer lyotropic cholesteric LC solutions and can be described by the following equation[17,19,20]

$$P = KC^{-\alpha} \qquad (2)$$

where C is the concentration, K is constant, and α is an exponent. From the data in Table 1, it can be calculated that the exponent α for the (E−CE)C/AA cholesteric LC

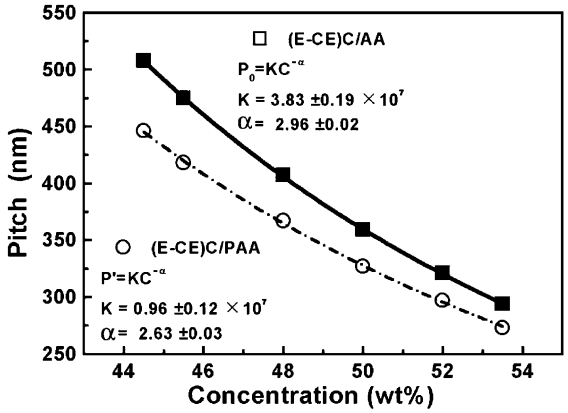

Figure 4. Curves of the pitch with concentration of the (E−CE)C/AA solutions and (E−CE)C/PAA composites.

solution is about 2.96 (Figure 4), i.e., P_0 varies inversely as almost the third power of the (E−CE)C concentration over a concentration range of 42−56 wt %. Besides, the wavelength is proportional to the pitch according to eq 1 and n can be regarded as a constant (the variation is less than 0.3%, Table 1); thus, λ_{max} also is inversely as the third power of the (E−CE)C concentration. In previous investigations in other polymer lyotropic cholesteric LC solutions, the exponent α is 3 for both the HPC/water[19] and acetoxypropylcellulose (APC)/acetone[20] cholesteric LC solutions whereas α is 2 for the poly-γ-benzyl-L-glutamate (PBLG)/dioxan cholesteric LC solution.[17] It should be mentioned that the power dependence of pitch with concentration for polymer lyotropic cholesteric LC solutions is dependent on the temperature,[20,21] and all the above results are determined at room temperature.[17,19,20] It is interesting that α values for the above cellulose cholesteric LC solutions, (E−CE)C, and HPC and APC solutions are equal, which may be derived from their same backbone, 1−4-linked β-D-glucose, and results in similar cholesteric structure and LC behavior.

From conformational energy calculations[22−24] and electron and X-ray diffraction,[25,26] all stable conformations of cellulose and its derivatives are rodlike extended helices, which is the first necessary condition of a polymer to form LC solution.[17−19,21] Furthermore, it has been confirmed by X-ray evidence that the rod-shaped molecules are arranged approximately parallel in the HPC[19] and its derivative[28] cholesteric LC solutions, even being arranged in a two-dimensional hexagonal array in the PBLG cholesteric LC solution,[17,18] when the concentration is above C_2.

WAXS diffraction spectra of the (E−CE)C/AA cholesteric LC solutions are presented in Figure 5. There are two strong diffraction peaks, and the peak at about 2θ = 20.5° represents an amorphous structure. The peak

Table 1. Structural Parameters and Optical Characters of the (E−CE)C/AA Cholesteric LC Solutions and (E−CE)C/PAA Cholesteric LC Composites

	(E−CE)C/AA solutions				(E−CE)C/PAA composites				
concentration (wt %)	λ_{max} (nm)	n	$P_0{}^a$ (nm)	2θ (deg)	λ_{max}(nm)	n	P^a (nm)	P^b (nm)	2θ (deg)
44.5	731	1.4522	508	8.040	657	1.4872	446	451	8.860
45.5	683	1.4525	475	8.120	615	1.4866	418	403	8.880
48.0	586	1.4534	407	8.180	543	1.4936	367	367	8.920
50.0	517	1.454	359	8.260	485	1.4967	327	330	8.940
52.0	463	1.4549	321	8.290	440	1.4985	297	304	8.960
53.5	424	1.4556	294	8.330	406	1.4993	273	272	8.980

[a] UV−Vis spectroscopy method, obtained by applying eq 1. [b] TEM method.

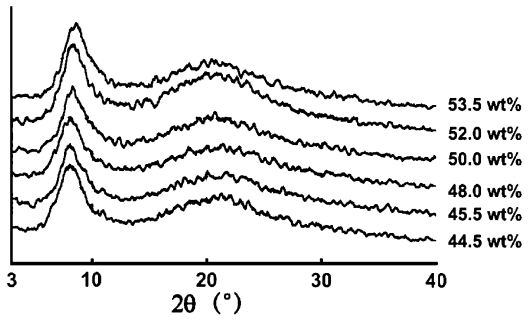

Figure 5. X-ray diffraction spectra of (E−CE)C/AA cholesteric LC solutions.

at about $2\theta = 8.2°$ is a characteristic X-ray diffraction peak of the cholesteric LC phase and is attributed to the average intermolecular distance (about 10.8 Å). As shown in Table 1, the value of the characteristic peak only very slightly increases with concentration, which results in the intermolecular distance decreasing slightly with the concentration (less than 3%).

On the basis of the X-ray diffraction results, the parallel packing model[17−19,28] is also fitted to the cholesteric structure of (E−CE)C/AA cholesteric LC solution, when the concentration is above C_2 (42 wt %). In the helical structure, the stiff (E−CE)C chains are arranged linear and parallel to each other within each "layer" (a small distance along the helix axis) and normal to the helix axis (Figure 1). AA molecules are dispersed in and interacted with the (E−CE)C chains by strong hydrogen bonding within a layer and between neighboring layers. Due to the bond length of the hydrogen bond and the volume of the (E−CE)C chains and AA, the average distance between the chains (d), a statistical distribution of the (E−CE)C chain distance of both within a plane and between neighboring layers, is fixed. Moreover, the side substituent groups in the (E−CE)C molecule, ethyl and cyanoethyl, are very short chains and cannot be folded. Thus, d just slightly decreases with increases in the concentration, and it coincides with the declining relationship between d and the concentration (all above C_2) found in PBLG,[17] HPC,[19] and APC[20,27] cholesteric LC solutions.

Effect of Polymerization on (E−CE)C/AA Cholesteric LC System. After photopolymerization of AA, it is found that the selective reflection property remains in the (E−CE)C/PAA composite (Figure 6a), and the shape and wavelength of the reflection peak remain with the sample's rotation (Figure 6b), which indicates the cholesteric order in the (E−CE)C/PAA composite retains the planar texture arrangement. However, comparing with that of the (E−CE)C/AA solution, λ_{max} of the (E−CE)C/PAA composite shifts shorter wavelengths (blue shift) after polymerization, as shown in Figure 6a. Besides the blue shift, the polymerization also causes a broad and intense decreased reflection band (Figure 6a), which results from some disorder in the cholesteric structure of the (E−CE)C/AA LC system.[29] Although the pitch of the (E−CE)C/PAA composites (P') is decreased consequently, according to eq 1 (Table 1), the relationship between the pitch and the (E−CE)C concentration is still found to follow eq 2 but α for the (E−CE)C/PAA composite decreases to 2.63 (Figure 4). From Figure 4, it is also found that the difference between P' and P_0, $P_0 - P'$, is decreased with the concentration. A similar result was observed in poly-γ-buzyl-L-glutamate/butyl acrylate (PbuLG/BuA) LC system by Tsutsui and Tanaka,[30] and the variation was proposed to be attributed to volume contraction of the solvent monomer.

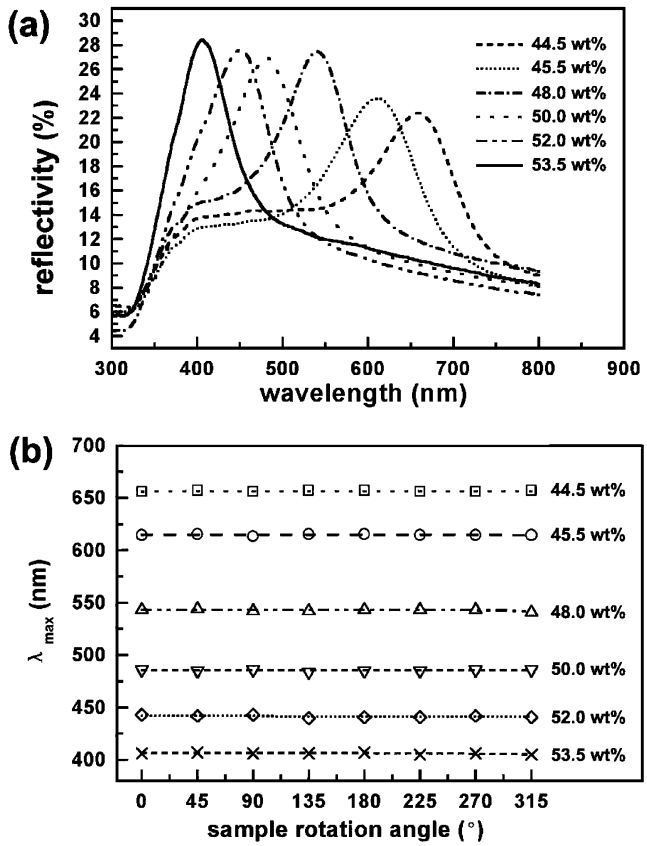

Figure 6. Reflection spectra of (E−CE)C/PAA cholesteric LC composite films (a) and λ_{max} with different sample rotation angles (b).

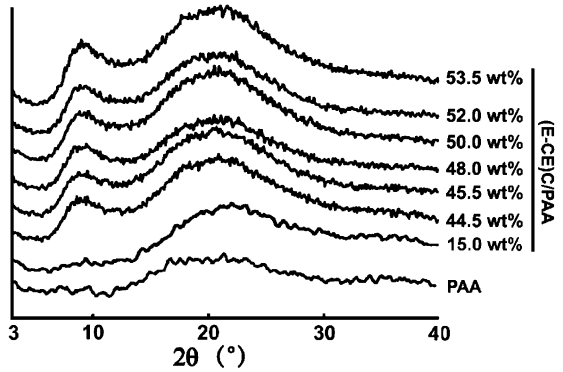

Figure 7. X-ray diffraction spectra of PAA and (E−CE)C/PAA composites. The PAA and lower concentration (E−CE)C/PAA composite (15 wt %) have no the characteristic peaks because there is no cholesteric structure when the (E−CE)C concentration is lower than the critical concentration.

The WAXS spectra of the (E−CE)C/PAA composites are shown in Figure 7. It was shown that the characteristic peak of the (E−CE)C/AA cholesteric LC system is retained after the polymerization of the AA, which also confirms that the cholesteric order in the (E−CE)C/AA LC solution is retained in the (E−CE)C/PAA composite. Similar to the variation of the reflection spectra, due to the effect of the polymerization, the intensity of the characteristic peak is decreased and has a shift to higher diffraction angles, which moves from about 8.2° to about 8.9° (d correspondingly changes to about 9.9 Å), as shown in Table 1. Moreover, the value of the peak

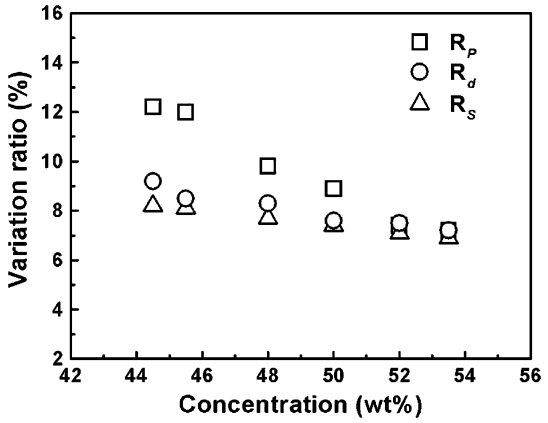

Figure 8. Plots of the variation ratio of the whole volume (R_S), the pitch (R_P), and the average intermolecular distance (R_d) with (E−CE)C concentration for the (E−CE)C/AA cholesteric LC system.

also keeps the slight increasing tendency with the concentration and results in the decline of the average intermolecular distance, d.

From the analysis of our experimental results it is concluded that λ_{max}, P, and d in the (E−CE)C/PAA composite all decreased compared with that in the (E−CE)C/AA solution, which are derived from the polymerization. As for the (E−CE)C/AA cholesteric LC system, although the whole volume contraction is not measured directly in this study, it can be roughly estimated by referring to the extent of volume contraction of AA monomer by polymerization. As for the pure AA, the volume contraction ratio is about 14.8% after polymerization at 0 °C. Thus, the whole volume contraction ratio of the system (R_S) is proportional to the volume fraction of AA, $R_S = (1 - C)14.8\%$, where C is the concentration of (E−CE)C. Figure 8 shows the (E−CE)C concentration dependence of R_S, the variation ratio of the average intermolecular distance, $R_d = (d_0 - d')/d_0$ (d_0 and d' are the d values before and after polymerization, respectively), and the variation ratio of the pitch, $R_P = (P_0 - P')/P_0$. R_d is very consistent with R_S, which indicates that the decrease of d directly results from the volume contraction of AA monomer, and the deviation between R_P and R_S is maybe due to the torsion angle's variation during the polymerzation.[30] Moreover, all three ratios show a steadily decreased tendency with (E−CE)C concentration, which indicates that the effect of polymerization on the (E−CE)C/AA cholesteric structure decreases with increases in (E−CE)C concentration, i.e., with increasing (E−CE)C concentration, the volume fraction of AA naturally decreases and, therefore, the effect of the volume contraction of the polymerization of AA on the (E−CE)C/AA LC system is decreased.

Lamellae and Defects in the (E−CE)C/PAA Composite TEM Micrograph. TEM study is carried out on the composite films that were microtomed perpendicular to the film surface. A periodical lamellar structure, which is a typical morphology of the macromolecular cholesteric phase and reflects the periodical variation of the molecular orientation in the cholesteric phase,[21−36] is observed in the microtomed sections of the (E−CE)C/PAA composite (Figure 9). Although the lamellar struc-

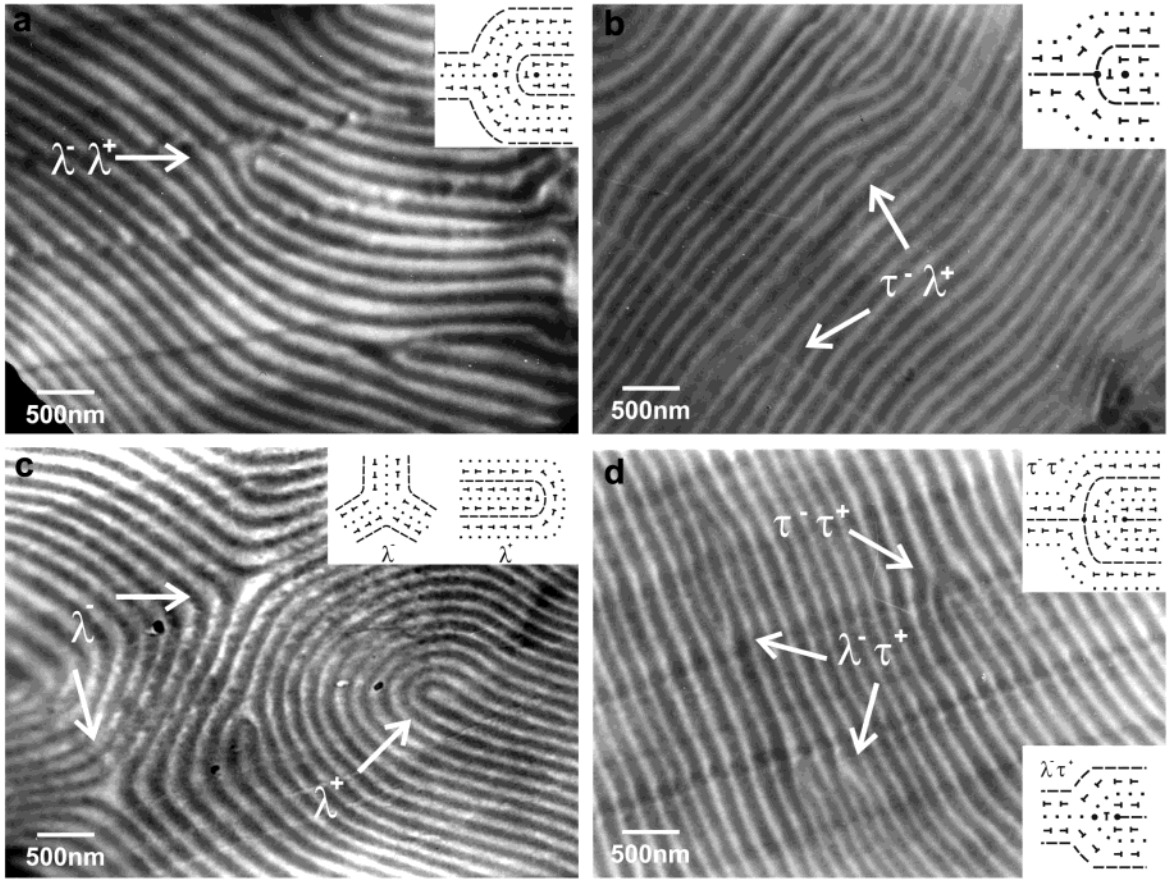

Figure 9. Lamellae structure and defects in the (E−CE)C/PAA composites TEM micrographs: (a) 45.5 wt %, (b) 50.0 wt %, (c) 52.0 wt %, and (d) 53.5 wt %. Arrows on the micrograph indicate some different defects. Dash, nail, and dot represent molecular director parallel, oblique, and normal to the plane, respectively.

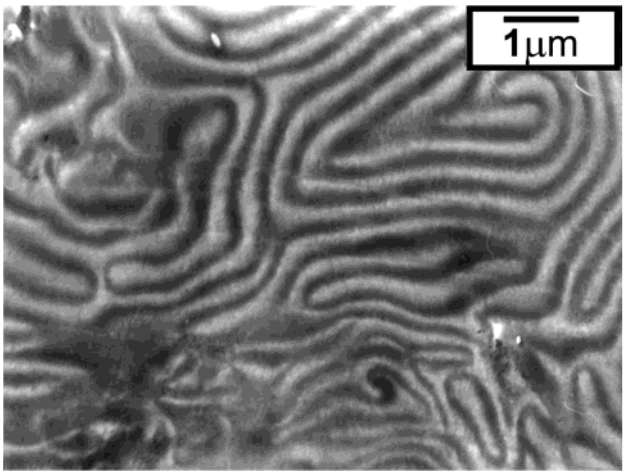

Figure 10. TEM micrographs of 37 wt % (E−CE)C/PAA cholesteric LC composite: dark and bright striations are random in the lamellae structure and have no fixed periodicity; more complicated defects are formed in the cholesteric structure.

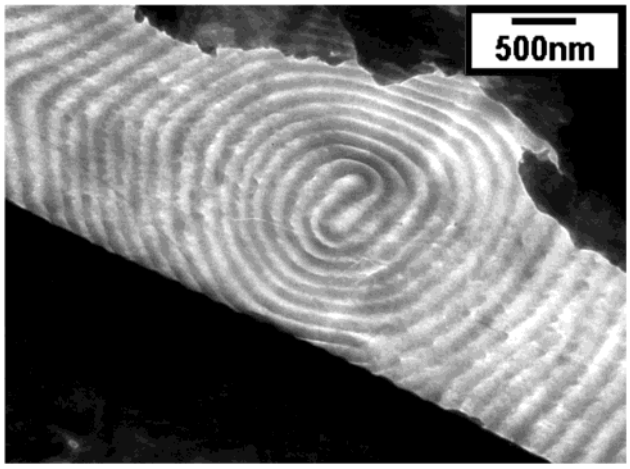

Figure 11. TEM micrographs of 50 wt % (E−CE)C/PAA composite with a bispirals pattern of spherulite texture.

tures observed by TEM has been debated on whether it is caused by electron irradiation, the results of investigations show that the orientation of the molecules is the main factor to cause image contrast.[34,35] The periodic corrugated surface in microtomed sections is generally thought to be due to preferential crack propagation as the sections are microtomed, which is relative to the orientation of the molecules, and thus producing a sinusoidal fracture surface.[34,35] Since the cholesteric structure in the (E−CE)C/AA solution is formed with the planar texture molecular arrangement when the concentration is in the range of 42−56 wt %, i.e., the cutting direction is parallel to the helix axes, the periodicity of the lamellar structure is equal to the half pitch ($P/2$). The pitch measured by the TEM method (P'') coincides with that calculated by reflection spectroscopy (P'), as shown in Table 1. It needs to be emphasized that the periodicity of the lamellar structure equals to the half pitch only when the cholesteric phase forms the planar texture, in which the helix axis lies in the micrograph plane. In low concentration (E−CE)C/AA solutions, smaller than 42 wt %, the mesophase generally forms focal conics or fan texture, in which the helix axes are random in the bulk. After sectioned perpendicular to the surface of the composite film, the lamellae have no fixed periodicity and the morphology is more complicated than that in the planar texture (Figure 10).

Besides the lamellae, defects or imperfections such as disclinations and dislocations of the cholesteric order are also important features in the cholesteric structure. The defects result from the singularity of the local director of the molecules and the singularity of the helix axis and are more complicated than those in the nematic state. According to the rotation axis conditions and the disclination line, there are different types defects in the cholesteric LC:[37] elementary disclinations (λ^-, λ^+, τ^-, and τ^+) and dislocations or disclination pairs ($\tau^-\lambda^+$, $\lambda^-\tau^+$, $\tau^-\tau^+$, and $\lambda^-\lambda^+$), as shown in Figure 9. Since the lower transmissibility of an electron beam makes a dark line on the TEM micrograph, the molecules on the dashed lines in the schematic models presumably lie parallel to the plane of the micrographs (normal to the defect lines).[32,34,35] Observed by TEM, it is found that the λ disclinations (Figure 9c) in the (E−CE)C/PAA composite appear more frequently than the τ disclinations and are often found individually in the domains, where the τ disclinations are rarely observed in individual form but are usually found in the disclination pairs. As shown in Figure 9, different pairs of disclinations are also observed in the (E−CE)C/PAA composite; it is found that the $\lambda^-\lambda^+$ type is more often observed in the micrographs, the $\tau^-\lambda^+$ and $\lambda^-\tau^+$ types are also found frequently, and the $\tau^-\tau^+$ type is observed only a few times, which hardly exists in the cholesteric structure.[32,38]

From above observations it is shown that the investigation method by combining the polymerizing solvent monomer technique and electron microscopy presents a visual way to study the structure in lyotropic cholesteric LC solution and offers much useful information, which is hardly observed by other methods such as polarized optical microscope (POM), etc. As shown in Figure 11, a bispirals pattern[16,18] of spherulite texture does not normally appear in the periodic lamellae of planar texture, which has not been observed before. To lyotropic cholesteric LC solution, the spherulite texture, which is formed by the strong interphases surface tension between the isotropic and LC phase, is the elementary mesophase texture formed among the isotropic phase when the concentration is above C_1. With increasing concentration, more LC molecules congregate in the LC phase and other advanced textures are consequently formed, such as the fingerprint texture, focal conic texture, planar texture, etc., and the spherulite texture would generally transform to other advanced textures and disappear, which due to the surface tension is too weak to keep the LC phase in the round shape. Thus, the TEM micrograph (Figure 11) offers new evidence to confirm that the advanced structures of the cholesteric, such as fingerprint texture and planar texture, are developed from the elementary form, a spherulite core.

Conclusion

In conclusion, structural characteristics and optical properties of the (E−CE)C/AA cholesteric LC system and the effect of the polymerization of AA on the system have been investigated. In the (E−CE)C/AA cholesteric solution, the maximum wavelength of the selective reflection (λ_{max}) and the pitch (P) varies inversely as the third power of the (E−CE)C concentration but the average intermolecular distance (d) only slightly decreases with (E−CE)C concentration. After polymeri-

zation of the solvent AA, the cholesteric order in the solution is well preserved in the (E−CE)C/PAA composites and the helix axes are retained in their original direction. λ_{max}, P, and d all decrease due to the volume contraction of AA; the effect of polymerization on the (E−CE)C/AA cholesteric structure decreases with increasing (E−CE)C concentration. In the fractured surface of the microtomed composites (parallel to the cholesteric helical axis), a periodic lamellar structure was observed by TEM. The periodicity of the lamellar structure is in good agreement with that obtained from the reflection method, equal to one-half of the cholesteric pitch. A series of defects (disclinations and dislocations) are also observed and elucidated from the TEM micrographs. It was found hat the λ-type disclination appears more frequently than the τ-type one, and some types of disclination pairs ($\tau^-\lambda^+$, $\lambda^-\tau^+$, and $\lambda^-\lambda^+$) are frequently observed, while the $\tau^{-\tau+}$ disclination pairs is observed a few times also.

Acknowledgment. Financial support by National Natural Science Foundation of China (Grant No. 29925411) is greatly appreciated.

References and Notes

(1) de Vries, H. *Acta Crysallogr.* **1951**, *4*, 219.
(2) Schadt, M.; Funfachilling, J. *J. Appl. Phys.* **1990**, *29*, 1974.
(3) Broer, D. J.; Mol, G. N.; van Haaren, J. A. M. M.; Lub, J. *Adv. Mater.* **1999**, *11*, 573.
(4) Palff-Muhoray, P. *Nature* **1998**, *391*, 745.
(5) Revol, J.-F.; Godbou, L.; Gray, D. G. *J. Pulp Paper Sci.* **1998**, *24*, 146.
(6) Pfaff, G.; Reynders, P. *Chem. Rev.* **1999**, *99*, 1963.
(7) Werbowyj, R. S.; Gray, D. G. *Mol. Cryst. Liq. Cryst.* **1976**, *34*, 97.
(8) Gray, D. G. *J. Appl. Polym. Sci., Appl. Polym. Symp.* **1983**, *37*, 179.
(9) Huang, Y. *J. Macromol. Sci., Polym. Phys. Ed.* **1989**, *B28*, 131.
(10) Jiang, S. H.; Huang, Y. *J. Appl. Polym. Sci.* **1993**, *50*, 607.
(11) Jiang, S. H.; Huang, Y. *J. Appl. Polym. Sci.* **1993**, *49*, 125.
(12) Huang, Y.; Jiang, S. H.; Shen, J. R. *Polym. Bull.* **1995**, *34*, 203.
(13) Huang, Y.; Loos, J.; Yang, Y. Q.; Petermann, J. *J. Polym. Sci., Polym. Phys.* **1998**, *36*, 439.
(14) Huang, Y.; Yang, Y. Q.; Petermann, J. *Polymer* **1998**, *39*, 5301.
(15) Zhang, Q.; Huang, Y. *Liq. Cryst.* **2002**, *29*, 289.
(16) Wang, L.: Huang, Y. *Macromolecules* **2002**, *35*, 3111.
(17) Robinson, C.; Ward, J. C.; Beevers, R. B. *Discuss. Faraday Soc.* **1958**, *25*, 29.
(18) Robinson, C. *Mol. Cryst.* **1966**, *1*, 467.
(19) Onagi, Y.; White, J.; Feller, J. *J. Polymer. Sci., Polym. Phys. Ed.* **1980**, *18*, 663.
(20) Tseng, S.-L.; Valente, A.; Gray, D. G. *Macromolecules* **1981**, *14*, 715.
(21) Uematsu, L.; Uemastu, Y. *Adv. Polym. Sci.* **1984**, *59*, 37.
(22) Ress, D. A.; Skerret, R. J. *Carbohydr. Res.* **1968**, *7*, 334.
(23) Pizzi, A.; Eaton, N. *J. Macromol. Sci., Chem.* **1968**, *A22*, 105.
(24) Simon, I.; Scheraga, H. A.; Manley, R. St. J. *Macromolecules* **1988**, *21*, 983.
(25) Zugenmaier, P. *Appl. Polym. Symp.* **1983**, *37*, 223.
(26) Steinmeier, H.; Zugenmaier, P. *Carbohydr. Res.* **1987**, *164*, 97.
(27) Laivins, G. V.; Gray, D. G. *Polymer* **1985**, *26*, 1435.
(28) Arici, E.; Greiner, A.; Hou, H.; Reuning, A.; Wendorff, J. H. *Macromol. Chem. Phys.* **2000**, *201*, 2083.
(29) Werbowyj, R. S.; Gray, D. G. *Macromolecules* **1984**, *17*, 1512.
(30) Tsutsui, T.; Tanaka, R. J. *J. Polym. Sci., Polym. Lett.* **1980**, *18*, 17.
(31) Costello, M. J.; Meiboom, S.; Sammon, M. *Phys. Rev. A* **1984**, *29*, 2957.
(32) Hara, H.; Satoh, T.; Toya, T.; Iida, S.; Orii, S.; Watanabe, J. *Macromolecules* **1988**, *21*, 14.
(33) Giasson, J.; Revol, J.-F.; Gray, D. G. *Macromolecules* **1991**, *24*, 1694.
(34) Bunning, T. J.; Vezie, D. L.; Lloyd, P. F.; Haaland, P. D.; Thomas, E. L.; Adams, W. W. *Liq. Cryst.* **1994**, *16*, 769.
(35) Boudet, A.; Mitov, M.; Bourgerette, C.; Ondarcuhu, T.; Coratger, R. *Ultramicroscopy* **2001**, *88*, 219.
(36) Arrighi, V.; Cowie, J. M. G.; Vaqueio, P.; Prior, K. A. *Macromolecules* **2002**, *35*, 7354.
(37) Kleman, M.; Fredel, J. *J. Phys. Colloq.* **1969**, *C4*, 43.
(38) Livolant, F. *J. Phys.* **1986**, *47*, 1605.

MA0344893